INFORMATICA, 2015, Vol. 26, No. 4, 593–620

DOI: http://dx.doi.org/10.15388/Informatica.2015.66

Helmholtz HSH-Based Basis: A Compact Phenomenological Representation of Arbitrary Reflectance

Shireen ELHABIAN[1,2]*, Aly FARAG[1]

[1]*Department of Electrical and Computer Engineering, University of Louisville, Louisville, KY 40217, USA*

[2]*Faculty of Computers and Information, Cairo University, Cairo, Egypt*

e-mail: s.elhabian@fci-cu.edu.eg, aly.farag@uofl.edu

Received: March 2015; accepted: June 2015

Abstract. Visual appearance can be phenomenologically modeled through an integral equation, known as *reflectance equation*. It describes the surface radiance which depends on the interaction between incident light field and surface *Bidirectional Reflectance Distribution Function* (BRDF). Being defined on the Cartesian product of the incident and outgoing hemispheres, hemispherical basis is the natural way to represent surface BRDFs. Nonetheless, due to their compactness in the frequency space, spherical harmonics have been extensively used for this purpose. Addressing the geometrical compliance of hemispherical basis, this paper proposes a Cartesian product of the hemispherical harmonics to provide a compact representation of plausible BRDFs, while satisfying the Helmholtz reciprocity property. We provide an analytical analysis and experimental justification that our basis provides better approximation accuracy when compared to similar bases in literature.

Key words: reflectance modeling, bidirectional reflectance distribution functions, spherical harmonics, hemispherical harmonics, Fourier-space representation.

1. Introduction

Various types of surfaces can be identifiable by their appearance which is the net result of the surface reflectance characteristics when exposed to illumination. Appearance models can be constructed using phenomenological models to capture surface appearance through mathematical modeling of the reflection process, leading to the *reflectance equation*. Using geometric optics, the reflectance equation, under the assumption of no surface emittance, is an integral equation describing the surface reflected radiance which results from the interaction between the incident light field and the surface bidirectional reflectance distribution function (BRDF).

A BRDF model can be obtained by (1) deriving an analytic formula based on either physical principles or simple formulation designed to mimic some kind of reflection, (2) simulating an assumed surface micro-geometry model, or (3) measuring BRDF values

*Corresponding author.

based on empirical observation. In all cases, it is required to devise a compact, yet accurate, BRDF representation of real-world materials which maintains the physical characteristics of surface reflectance. As such, BRDF representation has received much research attention from computer graphics and vision communities, where low-dimensional parametric models enable formulating inverse rendering problems as parameter estimation (Nishino and Lombardi, 2011).

A tabular representation, as simple as is, can be used to represent an arbitrary BRDF. However due to its four-dimensionality, full BRDF data are very scarce where the measurements can be restricted to the plane of incidence and is usually limited by some angular resolution. Further, the process of BRDF measurements acquisition could take hours to mechanically vary light source and sensor positions. Interpolation, extrapolation and smoothing are usually used to benefit from measured BRDF data in a convenient manner.

On the other end of the spectrum, analytic formula can present a very compact model for BRDF representation. Such formula can be either based on empirical observations, such as Lambertian model with a constant BRDF (Lambert, 1760) and Phong model (Phong, 1975; Blinn, 1977) (based on cosine-lobes), or physically based modeling of the microscopic surface geometry (i.e. distribution of micro-facet orientations) such as Torrance and Sparrow (1967) for rough specular surfaces and Oren and Nayar (1994) for rough diffuse surfaces. Despite the representation compactness, the lack of generality is the main drawback for such models, where there is no guarantee that these analytical models can represent arbitrary measured reflectance data, thus they only represent limited classes of surfaces.

On the middle ground, *phenomenological models* represent an arbitrary/real-world BRDF as a linear combination of a complete set of orthonormal basis functions, analogous to Fourier basis representing functions over the real line. Such low-dimensional representation has been used as an alternative to both measured/tabulated BRDFs and analytic models for three main reasons: First, most BRDFs are smooth functions (Westin *et al.*, 1992), i.e. they depend slowly on the directions and hence reflectance information is encoded via low frequency components. As such, they are considered as good candidates for representation using smooth orthonormal basis functions. Second, the human visual system is, in general, insensitive to appearance fine details (Ashikhmin and Premoz, 2006), i.e. high frequency components of surface reflectance, as long as features such as specularity and color are maintained. Matusik *et al.* (2003) supported this proposition by representing a BRDF as a linear combination of BRDF basis derived from densely sampled reflectance measurements of 100 real-world materials. Third, the lack of acquired data in areas such as near grazing angles, near retro-reflection directions (i.e. scattering in the backward direction) and along specular directions have justified the use of basis functions for BRDF representation to extrapolate missing BRDF measurements while filtering out violations of physical reflectance requirements.

Surface BRDFs are not arbitrary functions; in theory they are governed by basic principles of physics (Veach, 1997). (1) *Non-negativity*: A BRDF should attain non-negative values. (2) *Energy conservation*: A surface cannot reflect more light that it receives from the incident upper hemisphere. (3) *Reciprocity*: Helmholtz's law of reciprocity

(von Helmholtz, 1962) implies that the BRDF is invariant to permutation of incident and outgoing light directions. BRDF models which obey these principles are said to be *physically plausible BRDFs* (Lewis, 1994) since they can reproduce natural reflection (Montes and Urena, 2012), in contrast to non-physical ones which do not exist in nature. As such, devising a low-dimensional phenomenological model which yields physically plausible BRDFs goes to the heart of various vision and graphics applications.

The BRDF is a function defined on the Cartesian product of two hemispheres corresponding to the incident and outgoing directions; the natural way to represent such a hemispherical function is to use hemispherical basis. However, due to their compactness in the frequency space, spherical harmonics (SH) has been extensively used for this purpose (Cabral *et al.*, 1987; Westin *et al.*, 1992; Kautz *et al.*, 2002). Whereas SH is a complete set of orthonormal basis on the full unit sphere, hemispherical functions present discontinuities at the boundary of the hemisphere when represented in the spherical domain (Gautron *et al.*, 2004), demanding more coefficients for accurate representation.

The goal of this paper is thus to derive a low-dimensional, i.e. compact, phenomenological BRDF model which can: (1) address the physical compliance of the model to yield physically plausible BRDFs, (2) adhere to the geometrical nature of surface BRDF as being defined on a hemispherical domain rather than a spherical one, (3) address the trade-off between approximation accuracy and model compactness and (4) achieve accuracy comparable to the state-of-art phenomenological models. This suggests a linear model in terms of hemispherical orthonormal basis functions which obey symmetries such as isotropy and reciprocity. An inherent advantage of linear models is avoiding non-linear optimization processes used when employing polynomial functions (Montes and Urena, 2012). In particular, we propose a Cartesian product of the hemispherical harmonics (HSH) to provide a compact, yet accurate, representation for arbitrary BRDFs, while satisfying the physical characteristics of surface reflectance. We believe that our BRDF model can be used in place of simple Lambertian models in algorithms such as shape-from-shading and photometric stereo.

We assess the accuracy of our proposed basis functions analytically as well as numerically. We start off with a theoretical analysis of the representation accuracy of our model on different analytic physical BRDFs ranging from ideal diffuse and specular reflection to micro-facet based reflection models. We then evaluate the accuracy of our approximations using measured reflectance where scattered BRDF data might violate the Helmholtz reciprocity property.

2. Related Work

While several attempts adopted SH for BRDF representation, such models do not comply with the geometrical characteristics of non-emitting surface reflectance. For example, Kajiya and Herzen (1984) used SH to derive an analytical scattering function describing the radiation scattering in volume densities such as the case of clouds and fog. However this method used the wave theory of light as apposed to geometric optics. Cabral *et al.*

(1987) and Sillion *et al.* (1991) used such representation as a numerical approximation of the BRDF. In particular, assuming constant outgoing (*a.k.a.* viewing) direction, Cabral *et al.* (1987) derived SH coefficients for isotropic clamped BRDFs[1] based on a height field geometry without relying on neither analytic BRDF model nor measured reflectance data. They used a tabulated (binned) version of BRDFs while dividing the outgoing hemisphere into specific number of bins. This amounted for using smaller lookup tables while smoothing and interpolation took place. The hemispherical topology of reflectance was handled by replacing $\cos\theta_i'$ with the nonlinear term $\max(0, \cos\theta_i')$. While Cabral *et al.* (1987) used this representation for the purpose of simulating diffuse and glossy reflections of the environment, Sillion *et al.* (1991) tried to use such representation to solve the global illumination problem for arbitrarily complex reflectance models. By expanding the BRDF at fixed incoming direction, they represented the SH coefficients as functions of the incident angle which were stored as one dimensional cubic splines. Westin *et al.* (1992) simulated optical scattering to introduce a physically-based Monte Carlo algorithm to approximate arbitrary BRDFs. They used SH to define the basis over the Cartesian product of two spheres, taking the advantage of symmetry and reciprocity to reduce the non-zero coefficients representing the BRDF (isotropic as well as anisotropic ones). This representation does not require discretizing scattering directions as in the work of Cabral *et al.* (1987). The reciprocity property was enforced by using a combined SH basis function. The dependence on the incident and outgoing directions was encoded in a large matrix which stores the SH coefficients. On the other hand, to avoid on-the-fly evaluation of high-order basis functions, Kautz *et al.* (2002) parameterized the clamped BRDF by the outgoing direction to represent the 4D space of arbitrary BRDF (isotropic and anisotropic) in a 2D offline-table of SH coefficients.

On the other hand, several hemispherical basis have been proposed in literature to represent hemispherical functions. Sloan *et al.* (2003) used SH as in Westin *et al.* (1992) to represent an even-reflected (about xy-plane) version of a hemispherical function. Coefficients were found using least squares SH in contrast to Monte Carlo integration in Westin *et al.* (1992), however this leads to non-zero values in the lower hemisphere. Koenderink et al. (1996, 1998) used Zernike polynomials (Wyant and Creath, 1992), which are basis functions defined on a disk, to build hemispherical basis. Yet, such polynomials have high computational cost. Makhotkin (1996) and Gautron *et al.* (2004) proposed hemispherically orthonormal basis through mapping the negative pole of the sphere to the border of the hemisphere. Such contraction was achieved through shifting the adjoint Jacobi polynomials (Makhotkin, 1996) and the associated Legendre polynomials (Gautron *et al.*, 2004) without affecting the orthogonality relationship. Recently, Habel and Wimmer (2010) used the SH as an intermediate basis to define polynomial-based hemispherical basis. They used the SH basis functions which are symmetric to the $z = 0$ plane since they are orthogonal over the upper hemisphere. While other basis functions are shifted the same way that was proposed by Gautron *et al.* (2004). Although such basis definition leads to polynomial basis, this inhibit us from deriving an analytical expression of the harmonic expansion of the surface reflectance function and in turn of the irradiance integral.

[1] Clamped BRDF is the product of the BRDF with the foreshortening factor $\cos\theta_i'$.

In this work, we adopt the hemispherical harmonics (HSH) basis defined by Gautron *et al.* (2004) who used two HSH transformations to define hemispherical basis. Nonetheless, such definition does not guarantee Helmholtz reciprocity. On the other hand, Koenderink et al. (1996, 1998) used Zernike polynomials (Wyant and Creath, 1992) to define hemispherical basis which satisfy such a property, however such polynomials are known to have high computational complexity (Gautron *et al.*, 2004) and in the meantime, they are not defined for all combinations of polynomial orders and degrees. Thus, we provide an analytical analysis and experimental justification that for a given approximation order, our proposed HSH-based basis provide better approximation accuracy when compared to the Zernike-based ones (Koenderink and van Doorn, 1998), while, avoiding the high computational complexity inherent from Zernike polynomials (Gautron *et al.*, 2004).

3. Hemispherical Harmonics (HSH)

The HSH basis functions form a complete set of functions which are orthonormal over the surface of the unit hemisphere Ω, implying that any hemispherical smooth function can be expanded as an infinite series of these basis functions. The HSH can be defined as follows. An infinite series of *shifted* associated Legendre (SAL) polynomials $\{\widetilde{P}_n^m(x)\}$ can be used to express any piecewise continuous function over the interval [0, 1] where band-limited functions can be exactly reconstructed using finite number of polynomials. Thus any circular-symmetric function with no azimuthal dependence can be expressed in terms of SAL polynomials by mapping the polar angle θ to the interval [0, 1] using $x = \cos\theta$. It can be defined in terms of associated Legendre polynomials $\{P_n^m(x)\}$, defined in Eq. (1), as $\widetilde{P}_n^m(x) = P_n^m(2x - 1)$ after being linearly transformed to change the domain of the basis.

$$P_n^m(x) = \frac{1}{2^n n!}\left(1 - x^2\right)^{m/2} \frac{d^m}{dx^m} P_n(x), \quad n \geqslant 0,\ m \in [0, n], \tag{1}$$

where $\{P_n(x)\}$ is set of the Legendre polynomials which construct a complete, orthogonal set of functions over the interval $[-1, 1]$. These polynomials can be explicitly defined in terms of a power series defined as Arfken and Weber (2005),

$$P_n(x) = \sum_{k=0}^{\lfloor n/2 \rfloor} (-1)^k \frac{(2n - 2k)!}{2^n k!(n - k)!(n - 2k)!} x^{n-2k}, \tag{2}$$

where n denotes the polynomial order. The orthogonality relationship of the shifted associated Legendre polynomials is defined as Gautron *et al.* (2004),

$$\int_0^1 \widetilde{P}_n^m(x)\, \widetilde{P}_{n'}^m(x)\, dx = \frac{(n + m)!}{(2n + 1)(n - m)!} \delta_{nn'}. \tag{3}$$

In order to guarantee orthogonality in case of non-circular symmetric functions, shifted associated Legendre polynomials are combined with sinusoidal functions for the

azimuthal part dependency (Makhotkin, 1996). In case of circular-symmetric functions, zonal harmonics are used which reduce to the shifted associated Legendre polynomials with zero degree. The real HSH can be written as Gautron *et al.* (2004),[2]

$$H_n^m(\vec{\omega}) = H_n^m(\theta, \phi) = \widetilde{\Theta}_n^m(\theta)\Phi_m(\phi). \tag{4}$$

The *polar part* is given by $\widetilde{\Theta}_n^m(\theta) = \widetilde{N}_n^{|m|}\widetilde{P}_n^{|m|}(\cos\theta)$ where $\widetilde{P}_n^m = P_n^m(2z-1)$ is the shifted associated Legendre polynomials defined over the interval $[0, 1]$, the *azimuthal part* is defined in Eq. (6) and $\widetilde{N}_n^m$ being defined as the normalization factor,

$$\widetilde{N}_n^m = \sqrt{\frac{2n+1}{2\pi}\frac{(n-m)!}{(n+m)!}}, \tag{5}$$

$$\Phi_m(\phi) = \begin{cases} \sqrt{2}\cos(m\phi) & m > 0, \\ 1 & m = 0, \\ (-1)^m\sqrt{2}\sin(-m\phi) & m < 0, \end{cases} \tag{6}$$

where the harmonic order $n \geqslant 0$, the harmonic degree $m \in [-n, n]$, $\theta \in [0, \pi/2]$ and $\phi \in [0, 2\pi]$. By construction, the azimuthal part obeys the orthogonality condition such that,

$$\int_0^{2\pi} \Phi_m(\phi)\Phi_{m'}(\phi)\, d\phi = 2\pi\delta_{mm'}. \tag{7}$$

The orthonormality property connotes that,

$$\left\langle H_n^m(\theta, \phi), H_{n'}^{m'}(\theta, \phi)\right\rangle = \int_0^{2\pi}\int_0^{\pi/2} H_n^m(\theta, \phi)H_{n'}^{m'}(\theta, \phi)\sin\theta\, d\theta\, d\phi = \delta_{nn'}\delta_{mm'} \tag{8}$$

holds for real HSH, where $\delta_{nn'}$ denotes the Kronecker delta, i.e. $\delta_{nn'} = 1$ if $n = n'$ and 0 otherwise.

4. Proposed Helmholtz HSH-Based Reflectance Basis

The surface BRDF is defined as the ratio of the reflected radiance exiting along the outgoing direction $\vec{\omega}_o'$ to the surface irradiance incident from the incoming direction $\vec{\omega}_i'$, where both directions are defined with respect to the surface normal.[3] While it is often preferable to work with the clamped BRDF (Ramamoorthi, 2002), i.e. $f_r(\vec{\omega}_i', \vec{\omega}_o')\cos\theta_i'$, to enforce C^1 continuity at the equator and hence reduce the ringing in the approximation

[2]Note the difference between us and Gautron *et al.* (2004) in the factor of $(-1)^m$, since we preferred to include this factor in the harmonics definition rather than including it in the associated Legendre polynomial definition.

[3]Note that we use the primed coordinates to indicate measurements with respect to the local frame of a surface point.

(*a.k.a.* Gibbs phenomenon) (Sillion *et al.*, 1991), especially at grazing incident angles where singular performance is expected (Koenderink and van Doorn, 1998). Yet, we do not need to deal with the clamped BRDF since we are proposing hemispherical basis, i.e. we adhere to the geometrical structure of surface reflectance. In addition, clamped BRDF leads to a reflectance kernel which does not obey the reciprocity property. One way to handle this is to multiply both sides of the image irradiance equation by $\cos\theta'_o$ (Ramamoorthi, 2002), yet this inhibits us from modeling the image irradiance signal itself. As such, we opt for dealing with the BRDF itself without incorporating the foreshortening factor, $\cos\theta'_i$.

4.1. *Basis for Arbitrary Reflectance*

Consider the product of two HSH basis functions to give a mapping $\Omega'_i \times \Omega'_o \to \mathbb{R}$ from the Cartesian product of two hemispheres to the real line, one can define a combined basis function $H_p^q(\vec{\omega}'_i)H_r^s(\vec{\omega}'_o)$. Although these functions construct a complete orthogonal basis for the Cartesian product of two hemispheres, we are seeking a set of bases which span the subspace of functions characterized by maintaining the Helmholtz reciprocity property. Thus we define what we term *Helmholtz HSH-based basis* by symmetrizing the combined basis w.r.t. the incident and outgoing directions, i.e.

$$\mathcal{H}_{pr}^{qs}(\vec{\omega}'_i, \vec{\omega}'_o) = H_p^q(\vec{\omega}'_i)H_r^s(\vec{\omega}'_o) + H_r^s(\vec{\omega}'_i)H_p^q(\vec{\omega}'_o). \tag{9}$$

The orthogonality property of this basis is inherited from the orthonormality of the HSH basis in Eg. (8), where,

$$\langle \mathcal{H}_{pr}^{qs}(\vec{\omega}'_i, \vec{\omega}'_o), \mathcal{H}_{p'r'}^{q's'}(\vec{\omega}'_i, \vec{\omega}'_o)\rangle = 2\delta_{pp'}\delta_{qq'}\delta_{rr'}\delta_{ss'} + 2\delta_{pr}\delta_{qs}. \tag{10}$$

Hence, the *normalized* Helmholtz HSH-based basis can be defined as,

$$\mathcal{H}_{pr}^{qs}(\vec{\omega}'_i, \vec{\omega}'_o) = N_{pr}^{qs}\big[H_p^q(\vec{\omega}'_i)H_r^s(\vec{\omega}'_o) + H_r^s(\vec{\omega}'_i)H_p^q(\vec{\omega}'_o)\big], \tag{11}$$

where N_{pr}^{qs} is a normalization factor which guarantee the basis orthonormality. Using the orthogonality condition in Eq. (10), the normalization factor can be defined as,

$$N_{pr}^{qs} = \frac{1}{\sqrt{2 + 2\delta_{pr}\delta_{qs}}}. \tag{12}$$

Figure 1(d) visualizes up-to 3rd order of our proposed basis at a fixed incident direction (details about basis at fixed direction is given in Elhabian *et al.*, 2011). Thus, an arbitrary surface BRDF can be represented in terms of the Helmholtz HSH-based basis as follows,

$$f_r(\vec{\omega}'_i, \vec{\omega}'_o) = \sum_{p=0}^{\infty}\sum_{r=0}^{\infty}\sum_{q=-p}^{p}\sum_{s=-r}^{r} a_{pr}^{qs}\mathcal{H}_{pr}^{qs}(\vec{\omega}'_i, \vec{\omega}'_o). \tag{13}$$

In case of measured BRDFs, where scattered data are available, the Helmholtz reciprocity property might be violated. The process of projecting such scattered data on the

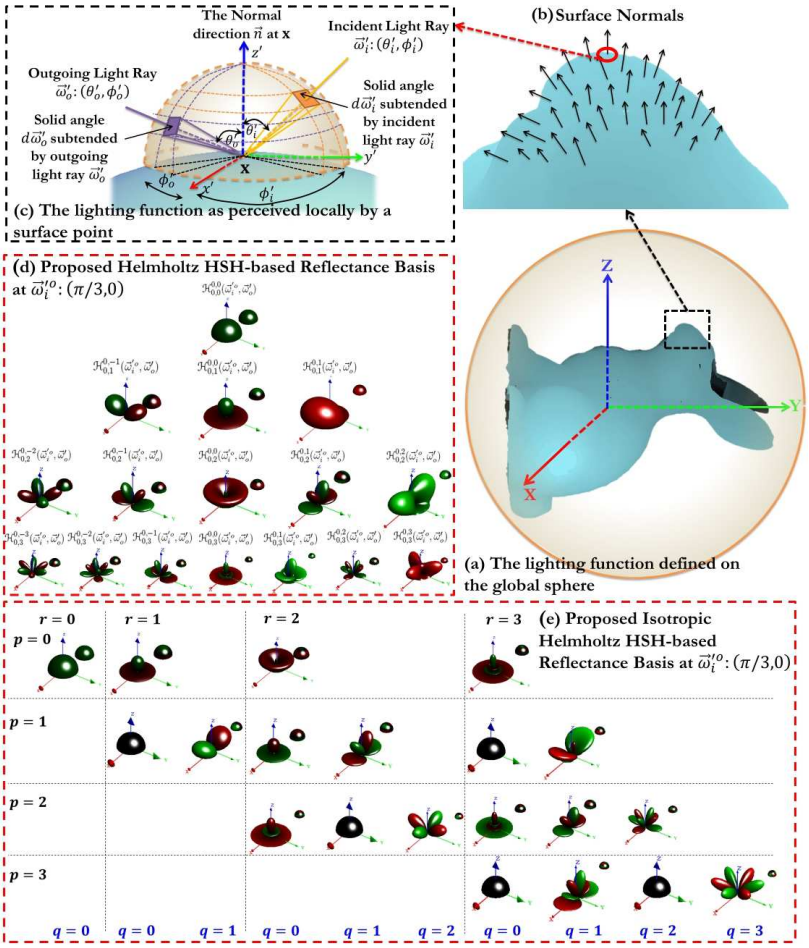

Fig. 1. (a) An object's surface is illuminated under distant lighting function defined on the global sphere. (b) An in-depth view of a surface patch showing surface normals at each surface point. Under the assumption of non-emitting surfaces, the reflection integral can be defined over the incident local hemisphere. (c) A zoom-in view at a surface point **x** seeing its surrounding world through a unit hemisphere Ω' centered at the point and oriented by the surface normal $\vec{n}$ at that point. Visualization of up-to 3rd order of the proposed anisotropic (d) and isotropic (e) Helmholtz surface reflectance basis at an incident direction $\vec{\omega}_i'$: $(\pi/3, 0)$. The order p runs from top to bottom while the associated order r runs from left to right. The azimuthal order q, or known as degree, also runs from left to right for each order r.

subspace spanned by the proposed basis filters out noisy components yielding the closest function which fits the data yet maintains the reciprocity property in the least-squares sense. The expansion coefficients of the series in Eq. (13) can be obtained through projecting the surface BRDF on the Helmholtz HSH-based basis such that,[4]

$$a_{pr}^{qs} = \left\langle f_r\left(\vec{\omega}_i', \vec{\omega}_o'\right), \mathcal{H}_{pr}^{qs}\left(\vec{\omega}_i', \vec{\omega}_o'\right)\right\rangle = \int_{\Omega_o'}\int_{\Omega_i'} f_r\left(\vec{\omega}_i', \vec{\omega}_o'\right)\mathcal{H}_{pr}^{qs}\left(\vec{\omega}_i', \vec{\omega}_o'\right) d\vec{\omega}_i'\, d\vec{\omega}_o'. \qquad (14)$$

[4]Complex conjugate is dropped since we are dealing with the real form of the basis.

By construction one has,

$$\int_{\Omega_o'}\int_{\Omega_i'} \mathcal{H}_{pr}^{qs}(\vec{\omega}_i', \vec{\omega}_o')\mathcal{H}_{p'r'}^{q's'}(\vec{\omega}_i', \vec{\omega}_o')d\vec{\omega}_i'\, d\vec{\omega}_o' = \delta_{pp'}\delta_{rr'}\delta_{qq'}\delta_{ss'}. \tag{15}$$

Hence, the BRDF energy content, which is defined as the integral $[f_r(\vec{\omega}_i', \vec{\omega}_o')]^2$ over its entire domain,[5] can be written as,

$$e_B = \int_{\Omega_o'}\int_{\Omega_i'} \left[f_r\left(\vec{\omega}_i', \vec{\omega}_o'\right)\right]^2 d\vec{\omega}_i'\, d\vec{\omega}_o' = \sum_{prqs} \left(a_{pr}^{qs}\right)^2. \tag{16}$$

Thus the approximation accuracy (or the energy captured by the Pth order approximation) can be defined as.

$$Acc_B(P) = \frac{\sum_{p=0}^{P}\sum_{r=0}^{P}\sum_{q=-p}^{p}\sum_{s=-r}^{r}\left(a_{pr}^{qs}\right)^2}{\int_{\Omega_o'}\int_{\Omega_i'}\left[f_r(\vec{\omega}_i', \vec{\omega}_o')\right]^2 d\vec{\omega}_i'\, d\vec{\omega}_o'}. \tag{17}$$

The list of the coefficients $\{a_{pr}^{qs}\}$ represents the bidirectional surface reflectance spectrum (BSRS) which characterize the BRDF in a manner similar to the Fourier spectrum, where low-order spectrum maintains the overall properties of the underlying kernel, whereas increasing the order adds more details.

For scattered reflectance data, high-order spectrum components would add noise rather than details (Koenderink and van Doorn, 1998), thus truncation/smoothing is mostly used to improve scattered data description. This resulting harmonic expansion defines a smooth function which can be considered as a least squares approximation of the underlying BRDF.

4.2. *Reflectance Basis for Isotropic Surfaces*

Isotropic BRDFs can be assumed when rotating the local tangent plane doesn't affect the surface reflectance properties, i.e. the BRDF becomes a function of only three variables $f_r(\vec{\omega}_i', \vec{\omega}_o') = f_r(\theta_i', \phi_i', \theta_o', \phi_o') = f_r(\theta_i', \theta_o', |\phi_o' - \phi_i'|)$. Thus depending only on $|\phi_o' - \phi_i'|$ allows negating both the incident and outgoing azimuthal angles without affecting the surface BRDF.

Furthermore, all terms in the harmonic expansion Eq. (13) vanish except for those terms which satisfy the isotropy assumption, i.e. rotational invariant w.r.t. the azimuthal part (adding $\Delta\phi'$ to both ϕ_i' and ϕ_o' makes no difference), this requires $q = s$. Hence the expansion coefficients of the BRDF are now defined, using three indices, by $a_{pr}^{qs} = a_{pr}^{qq} = a_{pr}^{(-q)(-q)} = a_{pr}^{q}$. From isotropy we have,

$$\begin{aligned}\mathcal{H}_{pr}^{qs}\left(\theta_i', \phi_i', \theta_o', \phi_o'\right) &= \mathcal{H}_{pr}^{qq}\left(\theta_i', \Delta\phi', \theta_o', 0\right) = \mathcal{H}_{pr}^{qq}\left(\theta_i', 0, \theta_o', \Delta\phi'\right) \\ &= \mathcal{H}_{pr}^{q}\left(\theta_i', \theta_o', \Delta\phi'\right),\end{aligned} \tag{18}$$

[5] Using the orthonormality property of the HSH-based basis, all terms in this integral vanishes except for $p = p'$, $q = q'$, $r = r'$ and $s = s'$.

where $\Delta\phi' = |\phi'_o - \phi'_i|$. Therefore, the harmonic expansion of isotropic BRDFs can be defined as,

$$f_r\big(\vec{\omega}'_i, \vec{\omega}'_o\big) = f_r\big(\theta'_i, \theta'_o, \Delta\phi'\big) = \sum_{p=0}^{\infty}\sum_{r=0}^{\infty}\sum_{q=-\min(p,r)}^{\min(p,r)} a_{pr}^{q}\mathcal{H}_{pr}^{q}\big(\theta'_i, \theta'_o, \Delta\phi'\big), \tag{19}$$

where the basis for isotropic surfaces can be defined in terms of the polar and azimuthal parts of the HSH as,

$$\mathcal{H}_{pr}^{q}\big(\theta'_i, \theta'_o, \Delta\phi'\big) = N_{pr}^{q}\big[\widetilde{\Theta}_{p}^{q}\big(\theta'_i\big)\widetilde{\Theta}_{r}^{q}\big(\theta'_o\big) + \widetilde{\Theta}_{r}^{q}\big(\theta'_i\big)\widetilde{\Theta}_{p}^{q}\big(\theta'_o\big)\big]\Phi_q\big(\Delta\phi'\big), \tag{20}$$

where

$$N_{pr}^{q} = N_{pr}^{qq}\Phi_q(0) = \frac{1}{\sqrt{2+2\delta_{pr}}}\begin{cases}\sqrt{2} & q > 0,\\ 1 & q = 0,\\ 0 & q < 0.\end{cases} \tag{21}$$

This reduced domain causes the number of independent spectrum components to be reduced drastically (Koenderink and van Doorn, 1998). The normalization factor for negative degree basis is zero, i.e. $N_{pr}^{q} = 0\ \forall q \in [-\min(p,r), -1]$. Moreover, due to the Helmholtz reciprocity, we have $\mathcal{H}_{pr}^{q}(.) = \mathcal{H}_{rp}^{q}(.)$. Thus the expansion in Eq. (19) can be rewritten as,

$$f_r\big(\vec{\omega}'_i, \vec{\omega}'_o\big) = f_r\big(\theta'_i, \theta'_o, \Delta\phi'\big) = \sum_{p=0}^{\infty}\sum_{r=0}^{p}\sum_{q=0}^{r} a_{pr}^{q}\mathcal{H}_{pr}^{q}\big(\theta'_i, \theta'_o, \Delta\phi'\big). \tag{22}$$

Whereas the isotropic bidirectional surface reflectance spectrum (IBSRS) can be obtained by,

$$a_{pr}^{q} = \int_{\Omega'_o}\int_{\Omega'_i} f_r\big(\theta'_i, \theta'_o, \Delta\phi'\big)\mathcal{H}_{pr}^{q}\big(\theta'_i, \theta'_o, \Delta\phi'\big)\, d\vec{\omega}'_i\, d\vec{\omega}'_o. \tag{23}$$

Figure 1(e) shows a visualization for up-to 3rd order of our proposed Helmholtz basis in case of isotropic surface BRDF. It can be observed that higher orders are entertained with larger number of basis adding more details to the BRDF representation. This in contrast to the isotropic basis proposed by Koenderink and van Doorn (1998) which maintains only 8 basis at the 3rd order representation due to the definition of the Zernike polynomials. This give insights that the proposed reflectance basis would capture similar energy content to that of the Zernike-based basis at lower orders of reflectance, leading to a more compact representation of surface BRDF. It is worth noting that we share the same number of orthonormal basis with Westin *et al.* (1992), Habel and Wimmer (2010), Gautron *et al.* (2004).

5. Representation of Analytic Reflectance Models

The approximating orders of the proposed reflectance basis expansion of an arbitrary BRDF primarily depend on the analytic form of the BRDF at hand, where smooth BRDFs require fewer coefficients for accurate representation compared to non-smooth/complex ones. In this section, we investigate the representation power of our proposed basis to approximate perfect diffuse and specular reflectance models. We also extend this analysis to investigate the spectrum of physical analytic models of surface reflectance such as Torrance–Sparrow specular reflection model (Torrance and Sparrow, 1967) for rough surfaces. Take note that we are mainly interested in physical (*a.k.a.* theoretical) models which try to accurately simulate reflectance using physics laws, as opposed to empirical models which provide a simple analytic formulation designed to mimic some reflection phenomena, e.g. (Phong, 1975; Blinn, 1977) models.

5.1. *Ideal Diffuse Reflectance*

Ideal diffuse, i.e. Lambertian, surfaces have the property that their BRDF is independent of the incoming and outgoing directions. The BRDF of a Lambertian surface is related to surface albedo ρ_d by a constant, i.e.,

$$f_r^L\big(\vec{\omega}_i', \vec{\omega}_o'\big) = \frac{\rho_d}{\pi}. \tag{24}$$

Since the Lambertian BRDF has no azimuthal dependence, it can be represented in terms of zonal-basis where $q = 0$. The isotropic surface reflectance spectrum, i.e. the expansion coefficients, can be obtained as follows:

$$\begin{aligned} a_{pr}^L &= a_{pr}^0 = N_{pr}^0 \frac{\rho_d}{\pi}\Bigg[\int_{\Omega_o'} \widetilde{\Theta}_r^0\big(\theta_o'\big)\, d\vec{\omega}_o' \int_{\Omega_i'} \widetilde{\Theta}_p^0\big(\theta_i'\big)\, d\vec{\omega}_i' \\ &\quad + \int_{\Omega_o'} \widetilde{\Theta}_p^0\big(\theta_o'\big)\, d\vec{\omega}_o' \int_{\Omega_i'} \widetilde{\Theta}_r^0\big(\theta_i'\big)\, d\vec{\omega}_i'\Bigg] \\ &= N_{pr}^0 \frac{\rho_d}{\pi}[\varsigma_r \varsigma_p + \varsigma_p \varsigma_r] = N_{pr}^0 \frac{2}{\pi}\rho_d \varsigma_r \varsigma_p, \end{aligned} \tag{25}$$

where,

$$\begin{aligned} \varsigma_p &= \int_{\Omega_o'} \widetilde{\Theta}_p^0\big(\theta_o'\big)\, d\vec{\omega}_o' \triangleq \int_{\Omega_i'} \widetilde{\Theta}_p^0\big(\theta_i'\big)\, d\vec{\omega}_i' \\ &= (-1)^p \sqrt{2\pi(2p+1)} \sum_{k=0}^{p} \frac{(-1)^k (p+k)!}{(k+1)(k!)^2 (p-k)!} \\ &= \begin{cases} 2.5066 & p = 0, \\ 0 & p > 0. \end{cases} \end{aligned} \tag{26}$$

Therefore, the only non-vanishing spectral component is at the zeroth-order, thus we only need one zero-order basis to construct the Lambertian reflectance kernel, scaled by[6]

$$a_{pr}^{L} = \begin{cases} \frac{\rho_d}{\pi} \varsigma_0^2 & p = 0,\ r = 0, \\ 0 & p > 1,\ 1 < r \leqslant p. \end{cases} \tag{27}$$

Thus the DC component of the BRDF spectrum is simply the Lambertian reflectance function, hence the Lambertian model is the lowest-order approximation of any reflectance function. This complies with the conclusion presented in Koenderink and van Doorn (1998).

5.2. *Ideal Specular Reflectance*

An ideal specular surface behaves like an ideal mirror, where radiance arriving along a particular incoming direction can only leave the surface along the specular direction $\vec{\omega}_s'$. This direction is obtained by reflecting the incoming direction about the surface normal at the point of interest. This implies that the outgoing polar angle θ_o' equals the incident polar angle θ_i' and the incident and outgoing rays lie in a plane containing the surface normal. According to Koenderink and van Doorn (1998), a specular reflectance kernel defined in Eq. (28) is used instead to define perfect mirror BRDF.

$$f_r^S\big(\theta_i', \phi_i', \theta_o', \phi_o'\big) \approx \frac{\delta(\theta_i' - \theta_o')\delta(\phi_i' - \phi_o' + \pi)}{\sin\theta_i'}. \tag{28}$$

The spectral components (expansion coefficients) of the mirror-like reflectance kernel can be obtained as follows.

$$\begin{aligned} a_{pr}^{S,qs} = & \int_{\phi_o'=0}^{2\pi} \int_{\theta_o'=0}^{\pi/2} \int_{\phi_i'=0}^{2\pi} \int_{\theta_i'=0}^{\pi/2} \delta\big(\theta_i' - \theta_o'\big)\delta\big(\phi_i' - \phi_o' + \pi\big) \\ & \mathcal{H}_{pr}^{qs}\big(\theta_i', \phi_i', \theta_o', \phi_o'\big) \sin\theta_o'\, d\theta_i'\, d\phi_i'\, d\theta_o'\, d\phi_o'. \end{aligned} \tag{29}$$

Since we are integrating over delta functions, the integral vanishes except for $\theta' = \theta_i' = \theta_o'$ and $\phi' = \phi_i' = \phi_o' - \pi$;

$$a_{pr}^{S,qs} = \int_{\phi'=0}^{2\pi} \int_{\theta'=0}^{\pi/2} \mathcal{H}_{pr}^{qs}\big(\theta', \phi', \theta', \phi' + \pi\big) \sin\theta'\, d\theta'\, d\phi'. \tag{30}$$

Due to the separability of HSH basis functions in Eq. (4), using Eq. (11), the integral can be factorized into polar and azimuthal parts as follows:

[6] $N_{00}^0 = 1/2$.

$$a_{pr}^{S,qs} = N_{pr}^{qs} \int_{\theta'=0}^{\pi/2} \widetilde{\Theta}_p^q(\theta') \widetilde{\Theta}_r^s(\theta') \sin\theta' \, d\theta' \times \left[\int_{\phi'=0}^{2\pi} \Phi_q(\phi') \Phi_s(\phi' + \pi) \, d\phi' + \int_{\phi'=0}^{2\pi} \Phi_s(\phi') \Phi_q(\phi' + \pi) \, d\phi' \right]. \quad (31)$$

According to the definition of the azimuthal part of the HSH in Eq. (6), we have the following relation,

$$\Phi_q(\phi + \pi) = \begin{cases} \Phi_q(\phi) & q \text{ is even}, \\ -\Phi_q(\phi) & q \text{ is odd}. \end{cases} \quad (32)$$

Therefore, the azimuthal part of the integral in Eq. (31) vanishes if q and s do not have the same parity, i.e. both are even or both are odd. Using the orthogonality of Φ_q functions in Eq. (7) leads to,

$$\int_{\phi'=0}^{2\pi} \left[\Phi_q(\phi') \Phi_s(\phi' + \pi) + \Phi_s(\phi') \Phi_q(\phi' + \pi) \right] d\phi' = \begin{cases} (-1)^s 2\pi \delta_{qs} & q + s \text{ even}, \\ 0 & q + s \text{ odd}. \end{cases} \quad (33)$$

Thus the integral in Eq. (31) can be written as,

$$a_{pr}^{S,qs} = \begin{cases} (-1)^s 2\pi \delta_{qs} N_{pr}^{qq} \int_0^{\pi/2} \widetilde{\Theta}_p^q(\theta') \widetilde{\Theta}_r^q(\theta') \sin\theta' \, d\theta' & q + s \text{ even}, \\ 0 & q + s \text{ odd}, \end{cases} \quad (34)$$

where

$$\int_0^{\pi/2} \widetilde{\Theta}_p^q(\theta') \widetilde{\Theta}_r^q(\theta') \sin\theta' \, d\theta' = \widetilde{N}_p^{|q|} \widetilde{N}_r^{|q|} \int_0^{\pi/2} \widetilde{P}_p^{|q|}(\cos\theta') \widetilde{P}_r^{|q|}(\cos\theta') \sin\theta' \, d\theta'. \quad (35)$$

Switching to the Cartesian representation, we have $z = \cos\theta'$, thus $dz = -\sin\theta' d\theta'$, while the integration domain changes from $[0, \pi/2]$ to $[1, 0]$. Using the orthogonality relation of the shifted associated Legendre polynomials in Eq. (3) and the definition of the normalization factor $\widetilde{N}_r^{|q|}$ in Eq. (5) yield,

$$\int_0^{\pi/2} \widetilde{\Theta}_p^q(\theta') \widetilde{\Theta}_r^q(\theta') \sin\theta' \, d\theta' = \left(\widetilde{N}_r^{|q|}\right)^2 \frac{(r + |q|)!}{(2r + 1)(r - |q|)!} \delta_{pr} = \frac{1}{2\pi} \delta_{pr}. \quad (36)$$

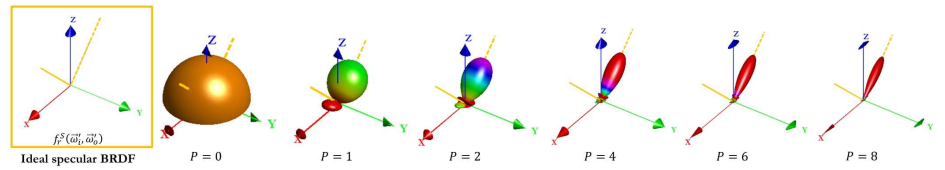

(a) Reconstruction of ideal specular *using our Helmholtz HSH-based basis* for different approximating orders

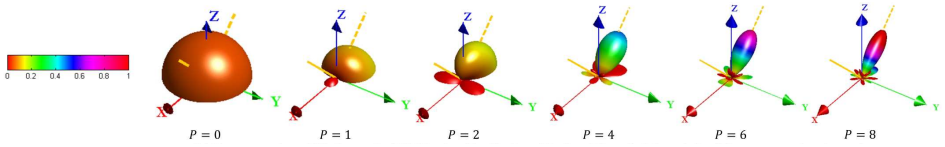

(b) Reconstruction of ideal specular *using Zernike-based basis* of Koenderink et al. for different approximating orders

Fig. 2. The reconstruction of the ideal specular reflectance kernel, where the light ray (in solid orange) is incident from direction $\theta_i' = \pi/4$ and $\phi_i' = 0$ and the perfect specular direction is plotted in dashed-orange. The approximating series has been truncated at different orders P, using (a) our proposed HSH-based basis, versus using (b) Zernike-based basis of Koenderink and van Doorn (1998).

Therefore, the spectral components of the mirror-like reflectance kernel can be written as,

$$a_{pr}^{S,qs} = \begin{cases} \frac{(-1)^q}{2}\delta_{pr}\delta_{qs} & q+s \text{ even}, \\ 0 & q+s \text{ odd}, \end{cases} \tag{37}$$

We can note that all non-vanishing spectrum components have the same absolute value, i.e. the specular reflectance kernel has a flat spectrum as an analogy to the Fourier spectrum of an impulse. The simplicity of the result originates from the assumption of ideal specular surface, however, such an expression becomes more complicated when taking into consideration the off-specular reflection for rough surfaces (Torrance and Sparrow, 1967).

Figure 2(a) plots the approximations of the ideal specular reflectance kernel obtained by truncating the infinite series in Eq. (13) at orders $P = 0, 1, 2, 4, 6$ and 8. For comparison purposes, Fig. 2(b) shows the approximation of the same kernel using the Zernike-based basis proposed by Koenderink and van Doorn (1998). In both case, the lowest order approximation leads to the Lambertian kernel, i.e. perfectly diffuse, where the reflected radiance is isotropically distributed and no specularity is observed. With higher orders, the radiance tends to reflect in the general direction of specularity, with narrower lobe.

It can be observed from Fig. 2 that with our HSH-based basis, the reflected radiance becomes more concentrated towards the specularity direction at lower orders when compared to the Zernike-based basis of Koenderink and van Doorn (1998), while being less sensitive to the abrupt truncation of the series causing less ringing effect. Further the reflected radiance have smaller spurious lobes in directions other than that of the perfect specular direction which vanish faster than that of the Zernike-based basis at higher orders.

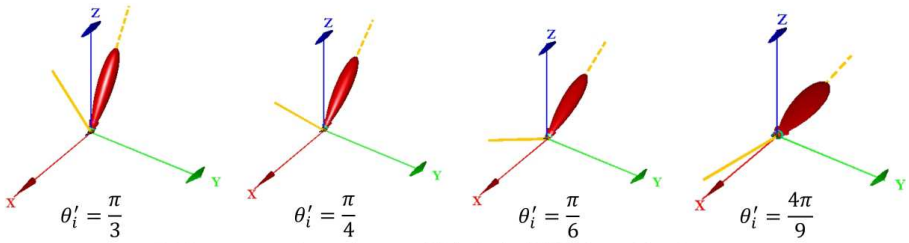

(a) Reconstruction using our Helmholtz HSH-based basis

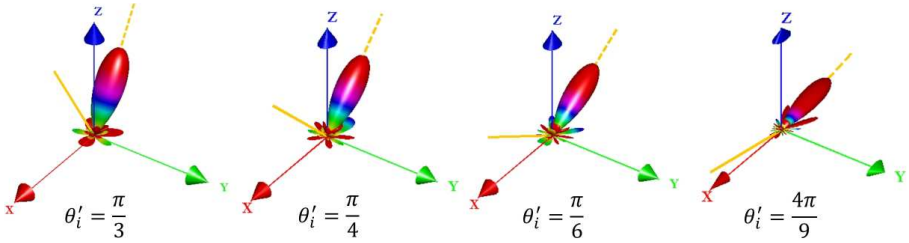

(b) Reconstruction using Zernike-based basis of Koenderink et al.

Fig. 3. The reconstruction of the ideal specular reflectance kernel, where the light ray (in solid orange) is incident from different directions and the perfect specular direction is plotted in dashed-orange. The approximating series has been truncated at order $P = 8$, using (a) our proposed HSH-based basis, versus using (b) Zernike-based basis of Koenderink and van Doorn (1998).

Figure 3 shows the reconstruction of the ideal specular lobe at different incident directions while truncating the approximating series at the 8th order. It is evident that our HSH-based basis provide a more compact approximation with lower ringing effect when compared to the Zernike-based basis.

It is important to note that, as in Fourier synthesis, the width of the reconstructed specular lobe primarily depend on the order at which the series is truncated where an infinite number of terms causes the reconstruction of the perfect specular spike. This leads to a relation between width and order.

Ideal specular surfaces rarely exist in the real world. Usually, radiation arriving in a particular direction leaves the surface in a small lobe of directions surrounding the specular direction, where the incoming radiance is shared over all outgoing directions within this lobe. This appears as a bright blob, also called specularity, along the specular direction. Phong model (1975) is commonly used to model the shape of the specular lobe, where the radiance leaving a specular surface is proportional to $\cos^l(\theta_o' - \theta_i')$, where θ_o' is the exit polar angle, θ_i' is the specular polar angle which is the same as the incident polar angle. l is a parameter defining the width of the specular lobe, where larger values of l defines narrower lobes and sharper specularities.

5.3. *Example of Non-Ideal Physical Reflectance Models*

Pure diffuse or specular surfaces are non-existent. Many surfaces can be approximated by having a BRDF consisting of a diffuse/Lambertian component and a specular component.

Diffuse albedo and specular albedo are used to weight these components respectively in this combination. The surface roughness model by Torrance and Sparrow (1967) is built on the assumption that the surface is composed of a collection of long symmetric V-cavities. Each V-cavity has two opposing facets with the width of each facet is much smaller than its length. The roughness of the surface is specified using probability function for the orientations of the facets. In order to use geometric optics, the area of each facet is assumed to be much larger than the wavelength of the incident light beam, and at the same time much smaller than the area of the surface patch being projected onto one pixel, thus the facets covered by one pixel can be described by statistical distributions.

The physically-based micro-facet model (TS) proposed by Torrance and Sparrow (1967) is focused on glossy reflectance, where the V-cavity geometry implies that only facets facing in direction of the halfway vector $\vec{\omega}'_h = (\theta'_h, \phi'_h)$ affect the BRDF, where the reflection from each facet is described by the Fresnel equation $F(\cos\theta'_h; \eta)$ where η is the classical refractive index from geometric optics. The fraction of the facets oriented in the direction of $\vec{\omega}'_h$ is described by a facet slope distribution function which rely on the surface's roughness. Whereas masking and shadowing of micro-facets are included in a geometric attenuation factor. For analytical simplicity, a simplified 4-parameter TS model is widely used in computer graphics, where the aforementioned model is modified in the following aspects while maintaining the physical properties of surface reflectance (Ramamoorthi and Hanrahan, 2001). The Fresnel for a refractive index η is normalized to be 1 at normal exitance. While F depends on the angle w.r.t. the half-way vector; in practice, this angle is very close to θ'_o, thus the Fresnel term becomes $F(\cos\theta'_o; \eta)/F(1; \eta)$. Ashikmin *et al.* (2000) believed that the distribution function has much greater impact on surface appearance than the geometric attenuation term, as such the geometric term can be omitted for simplicity (Ramamoorthi and Hanrahan, 2001). This also comply with the distribution-based BRDF (Ashikhmin and Premoz, 2006) where the shape of the reflection is dominated by the distribution function. Assuming, without loss of generality, that the viewer/camera is located at a distance relatively large compared to the object size such that the viewing direction coincides with the z-axis of the global reference frame; normal-exitance (i.e. $\theta'_o = 0$) can be used to approximate the imaging process. Thus the half-way angle can be written as $\theta'_h = \theta'_i/2$ (Ramamoorthi and Hanrahan, 2001) since there is no azimuthal dependance in the definition of TS-BRDF given by Torrance and Sparrow (1967). Hence the modified TS-BRDF can be written as,

$$f_r^{TS}(\vec{\omega}'_i, \vec{\omega}'_o) = \frac{\rho_d}{\pi} + \frac{\rho_s}{\pi\sigma^2 \cos\theta'_i \cos\theta'_o} \frac{F(\cos\theta'_o; \eta)}{F(1; \eta)} \exp\left[-\left(\frac{\theta'_i}{2\sigma}\right)^2 \right]. \tag{38}$$

Since there is no azimuthal dependance in Eq. (38), i.e. TS is radially symmetric, it can be expanded using zonal basis of the isotropic Helmholtz HSH-based basis of $\mathcal{H}^q_{pr}$, centered at surface normal $\vec{n}(\mathbf{x})$, where q is set to zero. The zonal basis can be written as,

$$\begin{aligned} \mathcal{H}^0_{pr}(\vec{\omega}'_i, \vec{\omega}'_o) = {} & \frac{1}{2\pi} \sqrt{\frac{(2p+1)(2r+1)}{2+2\delta_{pr}}} \\ & \times \left[\widetilde{P}_p(\cos\theta'_i) \widetilde{P}_r(\cos\theta'_o) + \widetilde{P}_r(\cos\theta'_i) \widetilde{P}_p(\cos\theta'_o) \right], \end{aligned} \tag{39}$$

where $\widetilde{P}_p$ is shifted associated Legendre polynomials (Gautron *et al.*, 2004) with order $p \geqslant 0$. Thus we can expand TS-BRDF in the subspace spanned by the isotropic Helmholtz HSH-based basis as,

$$f_r^{TS}(\vec{\omega}_i', \vec{\omega}_o') = \sum_{p=0}^{\infty} \sum_{r=0}^{\infty} a_{pr} \mathcal{H}_{pr}^0(\vec{\omega}_i', \vec{\omega}_o'). \tag{40}$$

The spectrum coefficients of the diffuse component of TS model can be derived using the orthogonality relation of the shifted associated Legendre polynomials, while their series representation can be used for the spectrum of the specular component. The spectrum coefficients can be obtained as,[7]

$$\begin{aligned} a_{pr}(\theta_o') &= \int_{\Omega_o'} \int_{\Omega_i'} f_r^{TS}(\vec{\omega}_i', \vec{\omega}_o') \mathcal{H}_{pr}^0(\vec{\omega}_i', \vec{\omega}_o')\, d\vec{\omega}_i'\, d\vec{\omega}_o' \\ &= 2\rho_d \delta_{p0} \delta_{r0} + \frac{\rho_s}{\pi \sigma^2 \cos\theta_o'} \frac{F(\cos\theta_o', \eta)}{F(1, \eta)} B_{pr}(\theta_o', \sigma), \end{aligned} \tag{41}$$

where,

$$B_{pr}(\theta_o', \sigma) = 2\pi \sqrt{\frac{(2p+1)(2r+1)}{2+2\delta_{pr}}} \left[\frac{\delta_{r0}}{2r+1} A_p(\theta_o', \sigma) + \frac{\delta_{p0}}{2p+1} A_r(\theta_o', \sigma) \right], \tag{42}$$

with

$$A_p(\theta_o', \sigma) = \int_0^{\pi/2} \frac{\sin\theta_i'}{\cos\theta_i'} \exp\left[-\frac{\theta_i'^2}{4\sigma^2} \right] \widetilde{P}_p(\cos\theta_i')\, d\theta_i'. \tag{43}$$

This means that $a_{p0} = a_{0p}$, thus we can use a single index for the spectrum coefficients where,

$$B_p(\theta_o', \sigma) = \begin{cases} 2\pi A_0(\theta_o', \sigma) & p = 0, \\ 2\pi \sqrt{\frac{2p+1}{2}} A_p(\theta_o', \sigma) & p > 0. \end{cases} \tag{44}$$

Hence TS-BRDF can be represented as,

$$f_r^{TS}(\vec{\omega}_i', \vec{\omega}_o') = a_0(\theta_o') + 2 \sum_{p=1}^{\infty} a_p(\theta_o') \mathcal{H}_{p0}^0(\vec{\omega}_i', \vec{\omega}_o'). \tag{45}$$

Note that the spectrum coefficients depends on the 4-parameters of TS model. Using Merl skin reflectance BRDF (Weyrich *et al.*, 2006) which provide TS parameters of six

[7] For proof refer to section 2 in the supplemental material.

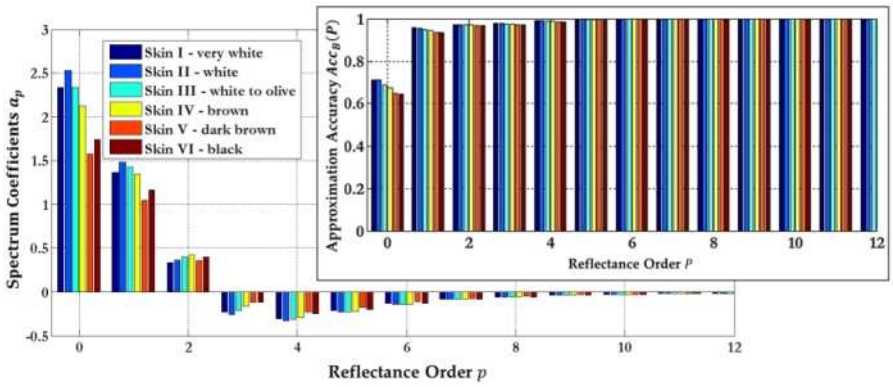

Fig. 4. A graphical representation of the first thirteen harmonic expansion coefficients of Torrance Sparrow reflection model under distant illumination using skin BRDF parameters of Merl Skin BRDF database (Weyrich *et al.*, 2006). Note that TS acts as a low pass filter, where the 5th order expansion is sufficient to encodes more than 99% of the BRDF energy content regardless of the skin type.

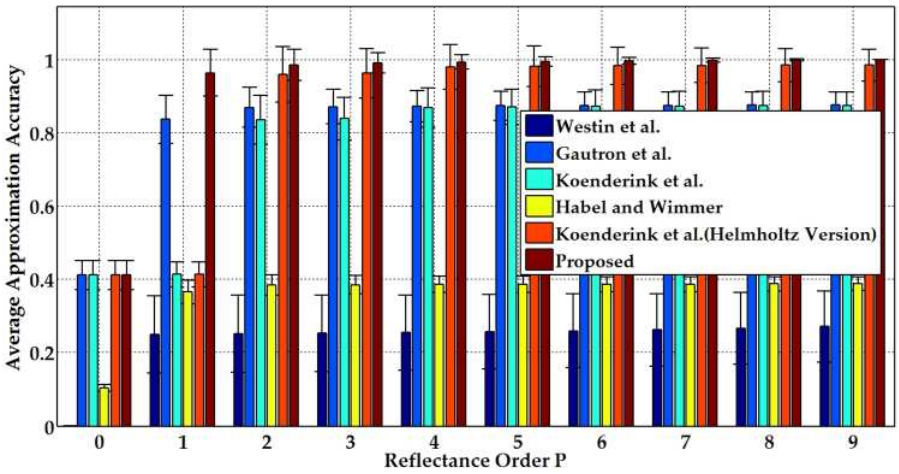

Fig. 5. The average approximation accuracy of Torrance Sparrow reflection model under distant illumination as a function of the truncating reflectance order P using skin BRDF parameters of Merl Skin BRDF database (Weyrich *et al.*, 2006).

different skin types (from very white to black), we investigate the harmonic spectrum in case of normal-exitance of each individual sample of skin BRDFs where Fig. 4 shows the graphical representation of the first thirteen coefficients (up to the 12th order) averaged over skin types. We also show the approximation accuracy, i.e. cumulative energy, of the pth order expansion as a function of the harmonic order. It can be observed that the spectrum of TS model decays along the harmonic order. While the approximation accuracy exceeds 99% using the 5th order approximation. It is worthwhile to note that more spectrum coefficients are needed due to the specular component of TS model, while the diffuse component is fully encoded in the zeroth order approximation.

Using the skin BRDF parameters of Merl Skin BRDF database (Weyrich *et al.*, 2006), Fig. 5 compares the average approximation accuracy of Torrance Sparrow reflection model

under distant illumination using our proposed isotropic basis in comparison to bases of Westin *et al.* (1992), Gautron *et al.* (2004), Koenderink and van Doorn (1998), Habel and Wimmer (2010), and the Helmholtz basis of Koenderink and van Doorn (1998) where we use their isotropic version. The average is taken over 100 samples for each skin type at different facial regions while the BRDF spectrum is obtained using Monte Carlo integration. While our basis provide a comparable accuracy to the Helmholtz basis of Koenderink and van Doorn (1998), one can observe that our proposed basis shows higher approximation accuracy especially at lower truncating reflectance orders compared to other bases. It is important to note that the spherical basis of Westin *et al.* (1992) shows the lowest accuracy compared to the hemispherical ones, this justifies the need of a representation which comply with the geometric structure of reflectance functions. As such, our basis provide a compact BRDF representation requiring fewer coefficients to accurately model surface BRDFs.

6. Modeling Scattered Reflectance Data

Scattered BRDF data might violate the Helmholtz reciprocity property; this can be filtered out through the process of projecting them onto the subspace spanned by our HSH-based basis, where the reciprocity property is preserved in the least-squares sense. Furthermore, in many practical cases, reflectance data are only available for plane-of-incidence geometries, where the incident and outgoing directions are coplanar with the surface normal. The reflectance spectrum components provide us with a phenomenological extrapolation from the available data in a unique manner (Koenderink and van Doorn, 1998). This is used implicitly when assuming a surface to be Lambertian with diffuse albedo obtained from few or even single measurements; this is equivalent to taking the zero-order approximation of the reflectance kernel. Thus using the reflectance spectrum components can be considered as a way of refining the reflectance kernel representation beyond the zero-order.

In this section, we further evaluate the accuracy and compactness of our HSH-based basis using BRDF measurements which are directly measured from real surfaces. We use BRDF databases which are available, free of charge, for academic purpose. In this paper, two BRDF databases are used for reflectance modeling. The first one is the database provided by Mitsubishi Electric Research Laboratories (Merl) (Matusik *et al.*, 2003) containing isotropic materials. The second one is offered by Columbia University and Utrecht University named as CUReT database (Dana *et al.*, 1999) containing a mix of isotropic and anisotropic materials.

6.1. *Experimentation on Isotropic-Merl Reflectance Data*

Merl reflectance data (Matusik *et al.*, 2003) is based on 100 isotropic materials to represent a wide variety of surface materials with different diffuse and specular reflection properties. Based on uniform spacing, 1,458,000 BRDF measurements are provided in 3D angular space using half-angle parameterization of Rusinkiewicz (1998). We use these BRDF samples as a lookup table since they are dense enough.

For each Merl material, Fig. 6 compares between the approximation accuracies provided by different *isotropic* reflectance bases in contrast to that of our proposed *isotropic* basis with different truncating reflectance orders P. The reflectance spectrum for each material is obtained by projecting randomly drawn Merl BRDF measurements using Monte Carlo integration onto the subspace spanned by our proposed *isotropic* basis in comparison to bases of Westin *et al.* (1992), Gautron *et al.* (2004), Koenderink and van Doorn (1998), Habel and Wimmer (2010) and the Helmholtz basis of Koenderink and van Doorn (1998) where we use their isotropic version. The sampling points are drawn from the Cartesian product of the incoming and outgoing (hemi)spheres (according to the basis definition). Some materials show extreme specular properties such as chrome-steel where it displays low approximation accuracies in Fig. 6(left) at lower reflectance orders regardless of the reflectance basis. In contrast, diffuse materials such as beige-fabric shows high approximation accuracies at lower reflectance orders. Nonetheless, in general, we can observe how our proposed basis provide the highest approximation accuracy for most of Merl materials especially at $P = 8$, while the spherical basis shows the worst accuracy for BRDF representation. These observations hold for both diffuse and specular materials. Figure 6 also shows the required minimum truncating reflectance order to achieve specific level of accuracy when using our isotropic basis. It can be noted that all Merl materials can be represented with accuracy of 95% with reflectance order less than or equal $P = 7$, while diffuse materials such as fabric materials can be represented with accuracy of 99% with reflectance order less than or equal $P = 4$.

6.2. *Experimentation on CUReT Reflectance Data*

The CUReT database (Dana *et al.*, 1999) consists of 61 BRDFs with sparse measurements of 205 measurements each over varying incident and outgoing directions. It also offers a BRDF parameter database which fits the sparse measurements to the Koenderink reflectance model (Koenderink and van Doorn, 1998). In our experimentation, we use the parameter database since the samples are not dense enough to be used directly as a BRDF lookup table. We opt to using the anisotropic parameters since this database contains anisotropic materials.

Figure 7 shows the approximation accuracy for each CUReT material for different truncating reflectance orders. The reflectance spectrum for each material is obtained by projecting randomly drawn CUReT BRDF measurements using Monte Carlo integration onto the subspace spanned by our proposed basis in comparison to bases of Westin *et al.* (1992), Gautron *et al.* (2004), Koenderink and van Doorn (1998), Habel and Wimmer (2010), and the Helmholtz basis of Koenderink and van Doorn (1998). Note that BRDF sparse measurements are interpolated at the drawn samples using the provided fitted measurements. The sampling points are drawn from the Cartesian product of the incoming and outgoing (hemi)spheres (according to the basis definition). It can be observed that our basis provide the best approximation accuracy levels for all CUReT materials especially with higher orders. It is again the spherical basis which provide the worst accuracy levels compared to the hemispherical ones. Notice that

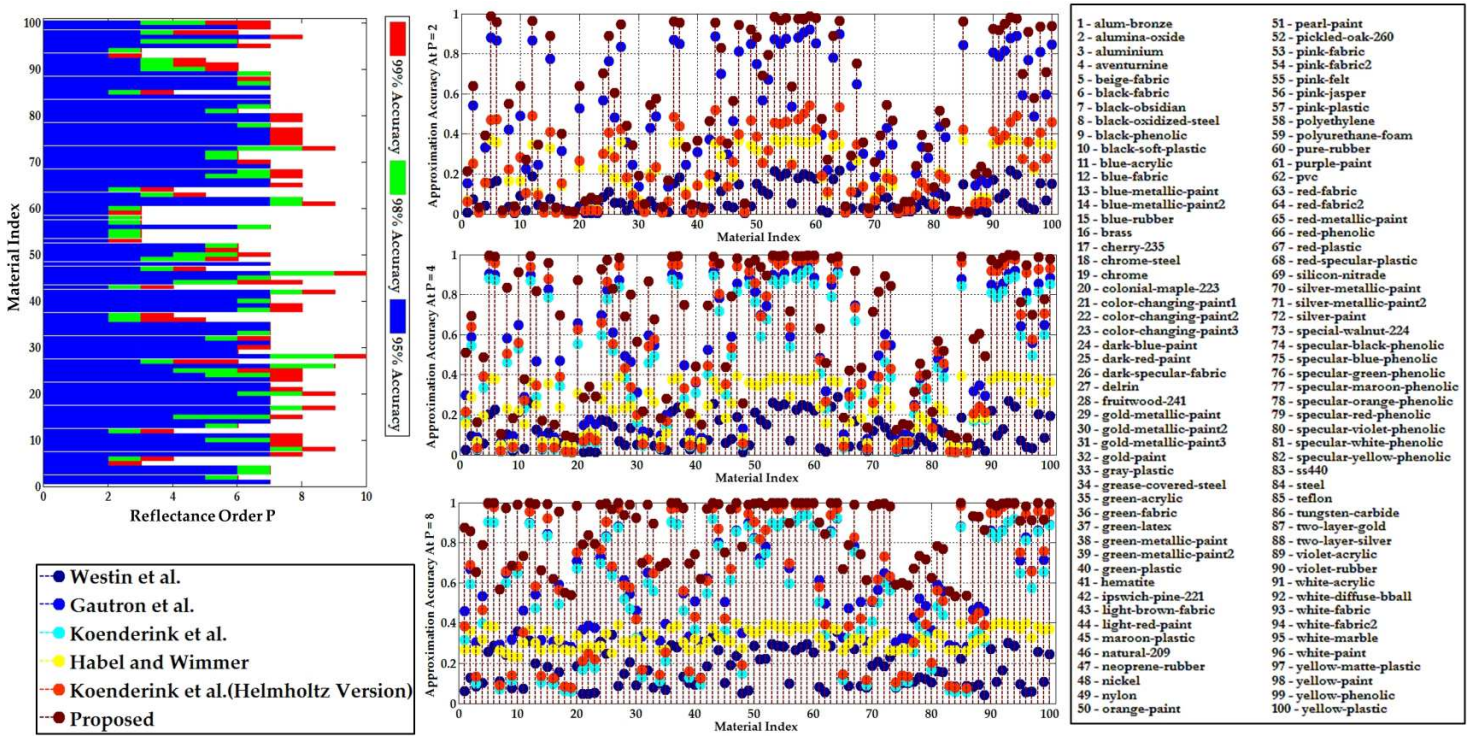

Fig. 6. Left: Required minimum reflectance order for the materials in the Merl database (Matusik *et al.*, 2003) when using our proposed *isotropic* basis. Right: The approximation accuracy of the materials (Matusik *et al.*, 2003) for different truncating reflectance orders P. It can be observed that our proposed basis provides the highest approximation accuracy for most of the Merl materials especially at reflectance order $P = 8$.

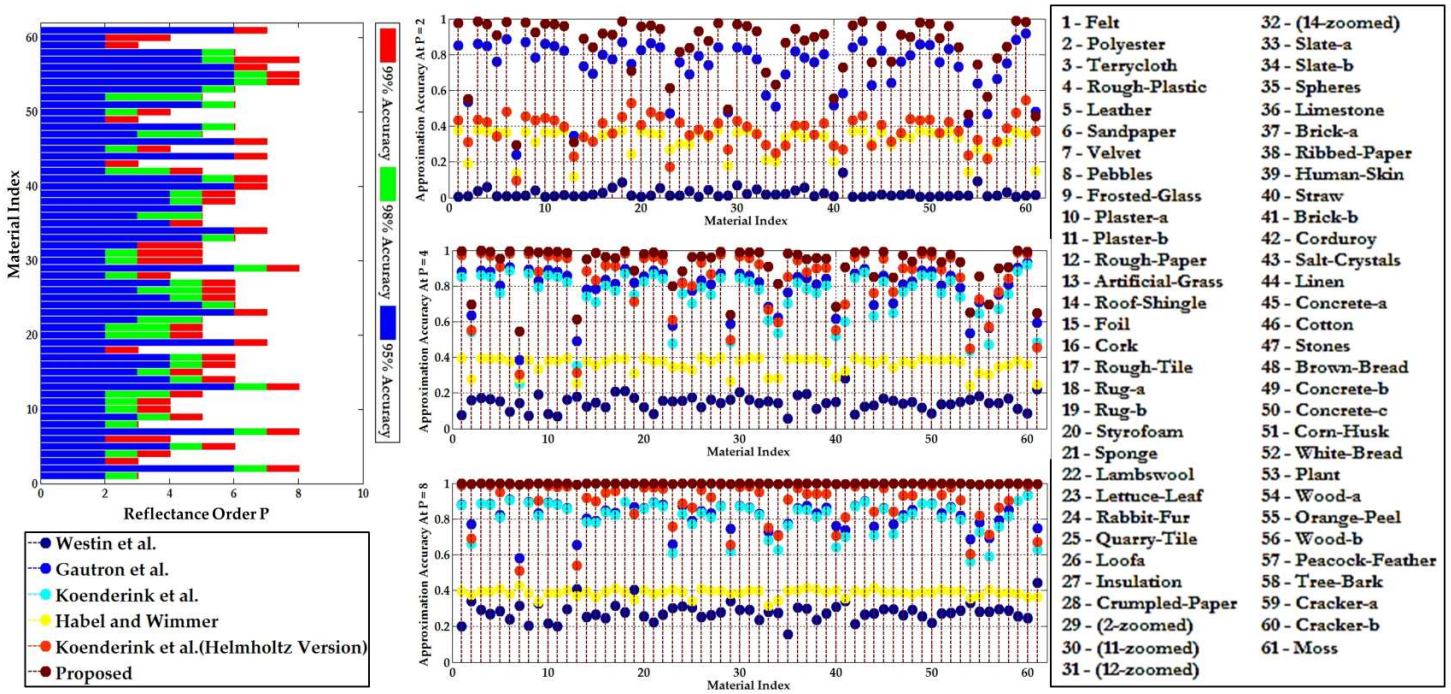

Fig. 7. Left: Required minimum reflectance order for the materials in the CUReT database (Dana *et al.*, 1999). Right: The approximation accuracy of the materials for different truncating reflectance orders P. It can be observed that our proposed basis provides the highest approximation accuracy for all CUReT, while the spherical basis (Westin *et al.*, 1992) provides the lowest accuracy compared to others.

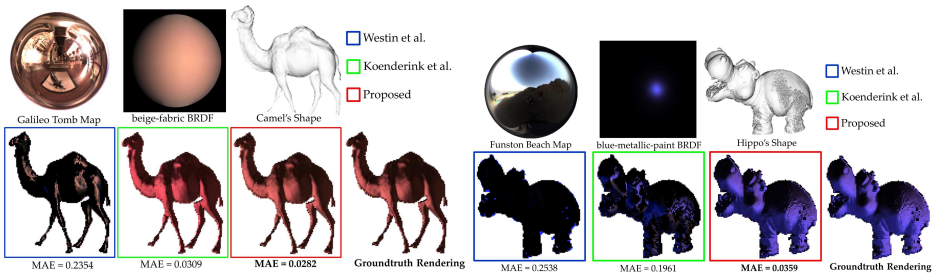

(a) (b)

Fig. 8. Sample of frequency-space rendering where the illumination order $N = 12$. Path tracing (Pharr and Humphreys, 2010) is used to render a unit sphere with the BRDF at the top-middle as well as the groundtruth rendering at the bottom-left. Mean absolute error (MAE) is shown below each rendered image where all intensities are normalized in the range $[0, 1]$. Note that the proposed basis capture the appearance of the surface reflectance under high-frequency illumination compared to the others.

an anisotropic material such as velvet is represented with higher approximation accuracy using the proposed basis when compared to others. Figure 7 also presents the required minimum truncating reflectance order to represent CUReT materials using our anisotropic basis where all the materials can be represented with accuracy of 99% with $P \leqslant 8$.

6.3. *Renderings*

In order to assess the representation accuracy of the proposed reflectance basis, we rendered images, in a similar manner as in Ramamoorthi and Hanrahan (2002), of the camel and hippo toys, respectively, of the "Weizmann Photometric Stereo Database" (Basri *et al.*, 2007). We fit the BRDF measurements up-to reflectance order $P = 8$ to (1) *spherical* harmonics basis (Westin *et al.*, 1992), (2) *hemispherical* Zernike-based basis (Koenderink and van Doorn, 1998) and (3) the isotropic version of the proposed reflectance basis. The main difference between the three types of basis is modeling the dependency of the surface BRDF w.r.t. the polar coordinates $\{\theta_i', \theta_o'\}$ where associated Legendre polynomials is used in (1) while Zernike polynomials and shifted associated Legendre polynomials in (2) and (3), respectively.

In Fig. 8(a), the image is rendered under a high-frequency illumination map (Galileo Tomp, Debevec, 1998) with a non-specular BRDF (beige-fabric, Matusik *et al.*, 2003) using irradiance harmonics of illumination order up-to $N = 12$. While in Fig. 8(b), the image is rendered under a low-frequency illumination map (Funston Beach, Debevec, 1998) with a specular BRDF (blue-metallic paint, Matusik *et al.*, 2003) using irradiance harmonics of illumination order up-to $N = 6$. It can be observed that spherical reflectance basis performs poorly at capturing the reflectance appearance while the proposed basis achieve lowest mean absolute error compared to the groundtruth rendering (achieved by path-tracing, Pharr and Humphreys, 2010).

7. Conclusion

This paper proposed a complete, orthonormal basis to provide a compact and efficient representation for surface bidirectional reflectance distribution function (BRDF), which is defined on the Cartesian product of two hemispheres. The proposed basis, which are defined in terms of hemispherical harmonics (HSH), preserve the Helmholtz reciprocity property of BRDFs while avoid the computational complexity inherited from Zernike polynomials that are usually used to construct hemispherical basis. An analytical as well as experimental justification was presented such that for a given truncating reflectance order, the proposed hemispherical basis provide better approximation accuracy of the BRDF when compared to similar bases in literature. While hemispherical basis provide higher approximation accuracies when compared to spherical ones, basis maintaining Helmholtz property was observed to provide higher accuracy levels compared to others. The closed form of the proposed basis was presented in case of isotropic and directional hemispherical reflectance. The proposed basis was further validated using scattered reflectance data which might violate the Helmholtz reciprocity property; where such property is maintained in the least-squares sense in the process of fitting the BRDF measurements to the HSH-based basis. Based on the fact that associated Legendre polynomials are defined for all combinations of polynomial order and degree in contrast to Zernike polynomials, HSH-based basis showed high BRDF approximation accuracy at lower orders. It was observed that the significance of BRDF parameters decayed with the approximation order versus the case of Zernike-based basis. It was shown that the proposed basis captured almost all diffuse and specular materials with reflectance order less than reflectance order $P = 10$.

References

Arfken, G., Weber, H. (2005). *Mathematical Methods for Physicists: A Comprehensive Guide*. 6th ed., Elsevier Academic Press – Mathematics, Chapter 12.

Ashikhmin, M., Premoz, S. (2006). Distribution-based brdfs. http://www.cs.utah.edu/~premoze/dbrdf/dBRDF.pdf.

Ashikmin, M., Premoze, S., Shirley, P. (2000). A microfacet-based brdf generator. In: *Proceedings of the 27th Annual Conference on Computer Graphics and Interactive Techniques (SIGGRAPH '00)*. ACM Press/Addison-Wesley Publishing Co., New York, NY, USA, pp. 65–74.

Barros, W., Carceroni, R., Coelho, L., Queiroz-Neto, J. (2007). An opto-mechanical apparatus for binocular Helmholtz stereopsis in static and dynamic scenes. In: *Brazilian Symposium on Computer Graphics and Image Processing (SIBGRAPI'07)*, pp. 213–220.

Basri, R., Jacobs, D., Kemelmacher, I. (2007). Photometric stereo with general, unknown lighting. *International Journal of Computer Vision*, 72(3), 239–257.

Belkasim, S., Ahmadi, M., Shridhar, M. (1996). Efficient algorithm for fast computation of Zernike moments. *Journal of the Franklin Institute*, 333(4), 577–581.

Blinn, J. (1977). Models of light reflection for computer synthesized pictures. *SIGGRAPH Computer Graphics*, 11(2), 192–198.

Cabral, B., Max, N., Springmeyer, R., (1987). Bidirectional reflection functions from surface bump maps. *SIGGRAPH Computer Graphics*, 21(4), 273–281.

Dana, K., Ginneken, B., Nayar, S., Koenderink, J. (1999) Reflectance and texture of real-world surfaces. *ACM Transactions on Graphics*, 18(1), 1–34.

Debevec, P. (1998). Rendering synthetic objects into real scenes: bridging traditional and image-based graphics with global illumination and high dynamic range photography. In: *Proceedings of the 25th Annual Conference on Computer Graphics and Interactive Techniques (SIGGRAPH '98)*. ACM, New York, NY, USA, pp. 189–198.

Elhabian, S., Rara, H., Farag, A. (2011). Towards efficient and compact phenomenological representation of arbitrary bidirectional surface reflectance. In: *Proceedings of the British Machine Vision Conference (BMVC)*. BMVA Press, pp. 89.1–89.11.

Gautron, P., Kriva'nek, J., Pattanaik, S., Bouatouch, K. (2004). A novel hemispherical basis for accurate and efficient rendering. In: *Proceedings of the Fifteenth Eurographics Conference on Rendering Techniques*. Eurographics Association, pp. 321–330.

Habel, R., Wimmer, M. (2010). Efficient irradiance normal mapping. In: *Proceedings of the 2010 ACM SIGGRAPH Symposium on Interactive 3D Graphics and Games*, pp. 189–195.

Hawkins, T., Einarsson, P., Debevec, P. (2005). A dual light stage. In: *Proceedings of the Eurographics Symposium on Rendering Techniques*, Eurographics Association, Konstanz, Germany, pp. 91–98.

Healy, D.M, Kostelec, P.J., Rockmore, D.N., Moore, S. (2003). FFTs for the 2-sphere-improvements and variations. *Journal of Fourier Analysis and Applications*, 9(4), 341–385.

Healy, D.M., Kostelec, P.J., Rockmore, D. (2004). Towards safe and effective high-order Legendre transforms with applications to FFTs for the 2-sphere. *Advances in Computational Mathematics*, 21(2), 59–105.

Kajiya, J., Herzen, B.V. (1984). Ray tracing volume densities. *SIGGRAPH Computer Graphics*, 18(3), 165–174.

Kautz, J., Sloan, P.-P., Snyder, J. (2002). Fast, arbitrary brdf shading for low-frequency lighting using spherical harmonics. In: *Proceedings of the 13th Eurographics Workshop on Rendering (EGRW '02)*. Eurographics Association, Aire-la-Ville, Switzerland, pp. 291–296.

Kintner, E. (1976). On the mathematical properties of the Zernike polynomials. *Optica Acta: International Journal of Optics*, 23(8), 679–680.

Koenderink, J., van Doorn, A. (1998). Phenomenlogical description of bidirectional surface reflection. *Journal of the Optical Society of America*, 15(11), 2903–2912.

Koenderink, J., Doorn, A. V., Stavridi, M. (1996). Bidirectional reflection distribution function expressed in terms of surface scattering modes. In: *European Conference of Computer Vision (ECCV)*. pp. 28–39.

Lambert, J., (1760). *Photometria sive de mensura de gratibus luminis colorum et umbrae*. Eberhard Klett.

Lewis, R., (1994). Making shaders more physically plausible. *Computer Graphics Forum*, 13(2), 109–120.

Lu, J., Little, J.J. (1999). Reflectance and shape from images using a collinear light source. *International Journal Computer Vision*, 32(3), 213–240.

Makhotkin, O. (1996). Analysis of radiative transfer between surfaces by hemispherical harmonics. *Journal of Quantitative Spectroscopy and Radiative Transfer*, 56(6), 869–879.

Matusik, W., Pfister, H., Brand, M., McMillan, L. (2003). A data-driven reflectance model. *ACM Transactions on Graphics*, 22(3), 759–769.

Mohammed, A., Jie, Y. (2002). Practical fast computation of Zernike moments. *Journal of Computer Science and Technology*, 17(2), 181–188.

Montes, R., Urena, C. (2012). *An overview of brdf models*. Technical report, Department Lenguajes y Sistemas Informaticos, University of Granada, Granada, Spain.

Nishino, K., Lombardi, S. (2011). Directional statistics-based reflectance model for isotropic bidirectional reflectance distribution functions. *Journal of the Optical Society of America A*, 28(1), 8–18.

Oren, M., Nayar, S. (1994). Generalization of Lambert's reflectance model. In: *Proceeding SIGGRAPH '94 Proceedings of the 21st Annual Conference on Computer Graphics and Interactive Techniques*. ACM, New York, pp. 239–246.

Pharr, M., Humphreys, G. (2010). *Physically Based Rendering: From Theory to Implementation*, 2nd ed.

Phong, B.T. (1975). Illumination for computer generated pictures. *Communications of the ACM*, 18(6), 311–317.

Prata, A., Rusch, W.V.T. (1989). Algorithm for computation of Zernike polynomials expansion coefficients. *Applied Optics*, 28(4), 749–754.

Ramamoorthi, R. (2002). A signal-processing framework for forward and inverse rendering. *PhD dissertation*. Stanford University, Stanford, CA, USA, Advisor(s) P. Hanrahan.

Ramamoorthi, R., Hanrahan, P. (2001). On the relationship between radiance and irradiance: determining the illumination from images of a convex Lambertian object. *Journal of the Optical Society of America A*, 18(10), 2448–2459. http://www.ncbi.nlm.nih.gov/pubmed/11583261.

Ramamoorthi, R., Hanrahan, P. (2002). Frequency space environment map rendering. *ACM Transactions on Graphics*, 21(3), 517–526.

Rusinkiewicz, S. (1998). A new change of variables for efficient BRDF representation. In: *Rendering Techniques '98, Proceedings of the Eurographics Workshop in Vienna, Austria, June 29–July 1, 1998*, pp. 11–22.

Sen, P., Chen, B., Garg, G., Marschner, S., Horowitz, M., Levoy, M., Lensch, H. (2005). Dual photography. In: *ACM SIGGRAPH 2005 Papers (SIGGRAPH '05)*. ACM, New York, NY, USA, pp. 745–755.

Sillion, F., Arvo, J., Westin, S., Greenberg, D., (1991). A global illumination solution for general reflectance distributions. *SIGGRAPH Computer Graphics*, 25(4), 187–196.

Sloan, P., Hall, J., Hart, J., Snyder, J., (2003). Clustered principal components for precomputed radiance transfer. *ACM Transactions of Graphics*, 22(3), 382–391.

Suda, R., Takami, M. (2002). A fast spherical harmonics transform algorithm. *Journal Mathematics of Computation*, 71(238), 703–715.

Tan, P., Mallick, S., Kriegman, D., Quan, L., Zickler, T., (2007). Isotropy, reciprocity and the GBR ambiguity. In: *Proceedings of IEEE Conference on Computer Vision and Pattern Recognition (CVPR)*. pp. 1–8.

Torrance, K., Sparrow, E., (1967). Theory for off-specular reflection from roughened surfaces. *Journal of American Optical Society*, 57(9), 1105–1114.

Veach, E., (1997). Robust Monte Carlo methods for light transport simulation. *PhD thesis*.

von Helmholtz, H., (1962). *Treatise on Physiological Optics*. Dover, New York, I, 231.

Westin, S., Arvo, J., Torrance, K., (1992). Predicting reflectance functions from complex surfaces. In: *Proceedings of SIGGRAPH*, ACM Press. pp. 255–264.

Weyrich, T., Matusik, W., Pfister, H., Bickel, B., Donner, C., Tu, C., McAndless, J., Lee, J., Ngan, A., Jensen, H., Gross, M., (2006). Analysis of human faces using a measurement-based skin reflectance model. *ACM Transactions on Graphics*, 25(3), 1013–1024.

Wyant, J., Creath, K., (1992) Basic wavefront aberration theory for optical metrology. *Applied optics and Optical Engineering*, 11(29), 2.

Zickler, T., Belhumeur, P., Kriegman, D., (2002). Helmholtz stereopsis: Exploiting reciprocity for surface reconstruction. *International Journal of Computer Vision*, 49(2), 215–227.

S. Elhabian received her BSc and MSc from Faculty of Computers and Information, Cairo University (FCI-CU), Egypt, in 2002 and 2005, respectively. She received her PhD in Electrical and Computer Engineering (ECE) from University of Louisville (UofL), USA, in Fall 2012. Since Fall 2002, she has joined FCI-CU as a teaching assistant. Since then she has earned professional as well as academic experience with more than 35 international peer reviewed publications including ICIP, ICCV, CVPR, CRV, MICCAI, ISBI and IET-CV. From 2007–2012, she was a graduate research assistant at Computer Vision and Image Processing (CVIP) Lab at UofL. During this time, she was involved in different research projects including pulmonary nodule detection and classification for the early diagnosis of lung cancer, volumetric representation of the corpus callosum for early detection of autism, illumination invariant image-based shape recovery and human face recognition. Elhabian also conducted teaching and mentoring undergraduate as well as graduate students in topics related to computer vision, image processing, signal processing and pattern recognition in FCI-CU and CVIP-UofL. She was awarded the best teaching assistant in Cairo University in 2005 and the outstanding ECE graduate student award at the University of Louisville in 2009. She has been selected, from a worldwide search to be among 30 of the best PhD candidates to participate in Computer Vision and Pattern Recognition (CVPR) Doctoral Consortium in 2012. Further, her PhD thesis received the UofL Graduate Dean's Citation award. Elhabian's research interests have been centered around computer vision and image understanding, including object detection and recognition, medical imaging, shape-from-X, statistical shape analysis, subspace learning and image formation modeling. In particular, she is fascinated with the implications of advances in these fields to society and industry.

A. Farag received the bachelor degree from Cairo University, Egypt and the PhD degree from Purdue University in electrical engineering. He joined the University of Louisville in August 1990, where he is currently a professor of electrical and computer engineering. At the University of Louisville, Dr. Farag founded the Computer Vision and Image Processing Laboratory (CVIP Lab) which focuses on imaging science, computer vision and biomedical imaging. Dr. Farag main research focus is 3D object reconstruction from multimodality imaging, and applications of statistical and variational methods for object segmentation and registration. He has authored or coauthored more than 250 technical papers in the field of image understanding, and coedited two volumes on Deformable Models for Biomedical Applications (Springer-Verlag 2007). He has applied his image understanding work to a number of industrial and biomedical applications including smart robotics, 3D reconstruction of the human jaw from video imaging, biomedical visualization, and in computer assisted early detection of lung and colon cancer. He holds a number of patents in these applications. Dr. Farag was an associate editor of the IEEE Transactions on Image Processing. He is a regular reviewer for the US National Science Foundation and the US National Institutes of Health, and various technical journals and international conferences. He is a senior member of the IEEE and SME. Dr. Farag was general co-chair of ICIP172009, and general chair of ICMT1711. He is Associate Editor for The British Computer Vision Journal IET-CV and author of the upcoming text on Statistical Modeling in Biomedical Imaging Analysis with Cambridge University Press.

Helmholco HSH bazė: kompaktiška fenomenologiška laisvojo atspindžio išraiška

Shireen ELHABIAN, Aly FARAG

Regimoji išvaizda gali būti fenomenologiškai modeliuojama integraline lygtimi, žinoma atspindžio lygties pavadinimu. Ši lygtis apibūdina paviršiaus spindesį, kuris priklauso nuo laisvojo šviesos lauko sąveikos su paviršiaus dvikryčio atspindžio skirstinio funkcija (DASF). Hemisferinė (pusrutulio) bazė natūraliai tinka aprašyti paviršiaus DASF, nes ji apibrėžiama kaip dekartinė krintančiosios ir grįžtančiosios hemisferų sandauga. Nepaisant to, šiam tikslui plačiai naudojamos sferinės harmonikos, išsiskiriančios kompaktiškumu dažnių srityje. Remiantis hemisferinės bazės geometriniu tinkamumu, šis straipsnis siūlo hemisferinių harmonikų Dekarto sandaugą kaip kompaktišką tikėtinų DASF išraišką, užtikrinančią Helmholco apgręžiamumo savybę. Analiziniais ir eksperimentiniais rezultatais pagrindžiamas siūlomos bazės didesnis aproksimavimo tikslumas lyginant su literatūroje pateikiamomis panašiomis bazėmis.